Circulation
circ.ahajournals.org

Circulation. **1995;**91:**2264-2273**
doi: 10.1161/01.CIR.91.8.2264

Articles

Table of Contents
Circulation. 1995;91:2264-2273

(*Circulation.* 1995;91:2264-2273.)

Articles

Comparison of In Vivo Tissue Temperature Profile and Lesion Geometry for Radiofrequency Ablation With a Saline-Irrigated Electrode Versus Temperature Control in a Canine Thigh Muscle Preparation

Hiroshi Nakagawa, MD, PhD; William S. Yamanashi, PhD; Jan V. Pitha, MD, PhD; Mauricio Arruda, MD; Xanzhung Wang, MD; Kenichiro Ohtomo, MD; Karen J. Beckman, MD; James H. McClelland, MD; Ralph Lazzara, MD; Warren M. Jackman, MD

From the Cardiovascular Section/Department of Medicine, University of Oklahoma Health Sciences Center and the Department of Veterans Affairs Medical Center, Oklahoma City.

Correspondence to Warren M. Jackman, MD, Department of Medicine/Cardiovascular Section, University of Oklahoma Health Sciences Center, PO Box 26901, Rm 5SP300, Oklahoma City, OK 73190-3048.

Abstract

Background It is thought that only a thin layer of tissue adjacent to the electrode is heated directly by electrical current (resistive heating) during radiofrequency ablation. Most of the thermal injury is thought to result from conduction of heat from the surface layer. The purpose of this study was to determine whether lesion depth could be increased by producing direct resistive heating deeper in the tissue with higher radiofrequency power, allowed by cooling the ablation electrode with saline irrigation to prevent the rise in impedance that occurs when the electrode-tissue interface temperature reaches 100°C.

Methods and Results In 11 anesthetized dogs, the thigh muscle was exposed and bathed with heparinized canine blood (36°C to 37°C). A 7F catheter, with a central lumen, a 5-mm tip electrode with six irrigation holes, and an internal thermistor, was positioned perpendicular to the thigh muscle and held at a constant contact weight of 10 g. Radiofrequency current was delivered to 145 sites (1) at high constant voltage (66 V) without irrigation (CV group, n=31), (2) at variable voltage (20 to 66 V) to maintain tip-electrode temperature at 80°C to 90°C without irrigation (temperature-control group, n=39), and (3) at high CV (66 V) with saline irrigation through the catheter lumen and ablation electrode at 20 mL/min (CV irrigation group, n=75). Radiofrequency current was applied for 60 seconds but was terminated immediately in the event of an impedance rise ≥10 Ω. Tip-electrode temperature and tissue temperature at depths of 3.5 and 7.0 mm were measured in all three groups (n=145). In 33 CV irrigation group applications, temperature was also measured with a separate probe at the center (n=18) or edge (n=15) of the electrode-tissue interface. In all 31 CV group applications, radiofrequency energy delivery was terminated prematurely (at 11.6±4.8 seconds) owing to an impedance rise associated with an electrode temperature of 98.8±2.1°C. All 39 temperature-control applications were delivered for 60 seconds without an impedance rise, but voltage had to be reduced to 38.4±6.1 V to avoid temperatures >90°C (mean tip-electrode temperature, 84.5±1.4°C). In CV irrigation applications, the tip-electrode temperature was not >48°C (mean, 38.4±5.1°C) and the electrode-tissue interface temperature was not >80°C (mean, 69.4±5.7°C). An abrupt impedance rise with an audible pop and without coagulum occurred in 6 of 75 CV irrigation group applications at 30 to 51 seconds, probably owing to release of steam from below the surface. In the CV and temperature-control group applications, the temperatures at depths of 3.5 (62.1±15.1°C and 67.9±7.5°C) and 7.0 mm (40.3±5.3°C and 48.3±4.8°C) were always lower than the electrode temperature. Conversely, in CV irrigation group applications, electrode and electrode-tissue interface temperatures were consistently exceeded by the tissue temperature at depths of 3.5 mm (94.7±9.1°C) and occasionally 7.0 mm (65.1±9.7°C). Lesion dimensions were smallest in CV group applications (depth, 4.7±0.6 mm; maximal diameter, 9.8±0.8 mm; volume, 135±33 mm^3), intermediate in temperature-control group applications (depth, 6.1±0.5 mm; maximal diameter, 11.3±0.9 mm; volume, 275±55 mm^3), and largest in CV irrigation group applications (depth, 9.9±1.1 mm; maximal diameter, 14.3±1.5 mm; volume, 700±217 mm^3; P<.01, respectively).

Conclusions Saline irrigation maintains a low electrode-tissue interface temperature during radiofrequency application at high power, which prevents an impedance rise and produces deeper and larger lesions. A higher temperature in the tissue (3.5 mm deep) than at the electrode-tissue interface indicates that direct resistive heating occurred deeper in the tissue (rather than by conduction of heat from the surface).

Key Words: catheter ablation • radiofrequency • arrhythmia • tachycardia

Introduction

Radiofrequency catheter ablation has become a principal form of therapy for paroxysmal supraventricular tachycardia and idiopathic ventricular tachycardia[1 2 3 4 5 6 7 8 9 10] and is being used in increasing numbers of patients for treatment of ventricular tachycardia associated with coronary artery disease and other forms of heart disease. Radiofrequency current delivered through a standard 7F 4-mm catheter tip electrode has been highly successful for ablation of arrhythmogenic tissue located within a few millimeters of the ablation electrode, such as accessory AV pathways (in patients with Wolff-Parkinson-White syndrome) and the atrial end of the slow AV-nodal pathway. However, in 1% to 10% of patients with accessory pathways and 30% to 50% of patients with ventricular tachycardia associated with a healed myocardial infarction, the arrhythmogenic tissue cannot be destroyed with a conventional ablation electrode.[11 12 13 14 15 16 17] Deeper lesions may be necessary for ablation in these patients.[18 19] For any given electrode size and tissue contact area, radiofrequency lesion size is a function of radiofrequency power

level and exposure time.[20 21] At higher power, however, the exposure time is frequently limited by an impedance rise that occurs when the temperature at the electrode-tissue interface reaches 100°C.[22 23] The impedance rise can be prevented by maintaining the electrode-tissue interface temperature at <100°C.

Two approaches have been used to prevent the impedance rise and maximize power delivery. In one approach, a thermistor is used in the ablation electrode to monitor tip-electrode temperature. The radiofrequency generator output is adjusted to deliver the greatest level of power that does not result in an increase in electrode temperature beyond a target value, such as 80°C.[24] This "temperature-control" approach is based on the findings that radiofrequency current delivered at conventional power directly heats only a thin layer of tissue adjacent to the electrode (since current density decreases at the second power of the distance from the electrode) and that most of the thermal lesion results from heat conduction from the thin surface layer.[25 26 27 28 29 30 31] These observations imply that the depth of the lesion is a function of the surface area that is heated, the temperature at the surface, and the time of surface heating.

The second approach to increase lesion size uses a very large ablation electrode (8F, 8 to 10 mm in length).[32] The larger electrode-tissue contact area results in a greater volume of direct resistive heating.[29] In addition, the larger electrode surface area exposed to the blood results in greater convective cooling of the electrode by the blood. This cooling effect helps to prevent an impedance rise, allowing longer application of radiofrequency current at higher power, which produces a larger, deeper lesion. The two principal limitations of a large ablation electrode (8 to 10 mm in length) are the reduction in mobility and flexibility of the catheter (which may impair positioning of the ablation electrode) and a reduction in the resolution of recordings from the ablation electrode (making it more difficult to identify the optimal ablation site).

An alternative approach, originally proposed by Wittkampf et al,[33 34] is to irrigate the ablation electrode with saline for convective cooling to maintain a low electrode-tissue interface temperature and prevent an impedance rise. Since convective cooling from the bloodstream is not required, an irrigated electrode may be capable of delivering higher radiofrequency power at sites of low blood flow, such as within a ventricular trabecular crevasse. Other theoretical advantages of an irrigated electrode versus a very large ablation electrode include a more flexible catheter and higher-resolution recordings for more accurate mapping.

The purpose of this study is to compare the tissue temperature profile in vivo and lesion geometry between radiofrequency ablation at high power in which a saline-irrigated electrode (active cooling) is used with radiofrequency ablation in which variable output to maintain constant electrode temperature (80°C to 90°C), ie, temperature-control, is used.

A novel canine thigh muscle preparation was used to allow in vivo measurement of tissue temperature at various depths during the application of radiofrequency current. The hypothesis being tested is that direct resistive (electrical) heating is not necessarily limited to a thin surface layer. If radiofrequency power can be increased sufficiently by preventing an impedance rise (by maintaining a low temperature at the electrode-tissue interface), direct resistive heating may occur several millimeters below the surface and significantly increase lesion depth.

Methods

Experimental Preparation

The experimental protocol was approved by the University of Oklahoma Committee on Use and Care of Animals. Eleven mongrel dogs weighing between 18 and 22 kg were anesthetized with 25 mg/kg sodium pentobarbital and ventilated mechanically with room air. General anesthesia was maintained with supplemental doses of sodium pentobarbital. Each dog was placed on its left side. The right carotid artery was cannulated for continuous monitoring of arterial pressure. A 15-cm skin incision was made over the right thigh muscle (Fig 1). The skin, overlying connective tissue, and thin superficial muscle were gently dissected, exposing the surface of the thicker underlying muscle. The fascia on the surface of the muscle was usually thin and transparent. Any thicker fascia was removed. The edges of the skin were raised to form a cradle that was filled with heparinized canine blood at 36°C to 37°C (Fig 1). The blood was exchanged at a flow rate of 20 mL/min.

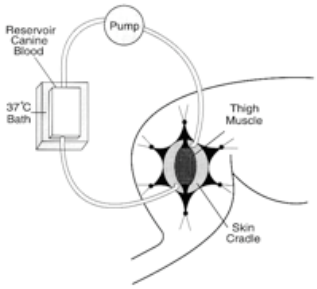

View larger version (31K):
In this window
In a new window

Figure 1. Schematic of the thigh muscle preparation. The skin, connective tissue, and thin superficial muscle are dissected to expose the smooth, glistening surface of the thick thigh muscle. The edges of the skin were raised to form a cradle, which was filled with heparinized canine blood (36°C to 37°C) that was exchanged at 20 mL/min.

A specially designed 7F deflectable quadripolar electrode catheter with a central lumen (Cordis Webster, Inc) was used. The tip electrode was 5 mm long and had six 0.4-mm-diameter irrigation holes located radially around the electrode, 1 mm from the tip (Fig 2). The tip electrode also contained a thermistor, 2.5 mm from the tip, allowing measurement of the tip-electrode temperature between 20°C and 120°C with an accuracy of ±2°C. The catheter was positioned perpendicular to the thigh muscle, and the tip electrode was held in contact with the thigh muscle at a constant weight of 10 g by use of a custom balance (Fig 2). Tissue temperatures were measured with fluoroptic thermal probes (Luxtron model 3000; measurement range, 0°C to 125°C; accuracy, ±0.2°C). The fluoroptic temperature measurement system was equipped with a radiofrequency-shielded package designed to prevent fluctuations of averaged temperatures >0.2°C root-mean-square (RMS) in stray radiation fields of up to 10 mW/cm^2 (1966 American National Standards Institute standard). Two thermal sensor probes were bundled together with shrink tubing. One sensor tip extended 3.5 mm from the end of the shrink tubing, and the other sensor tip extended 7.0 mm. The sensor probes were inserted into the muscle (3.5 and 7.0 mm from the surface) directly adjacent to the ablation electrode (Fig 2). In 3 of the 11 dogs, an additional fluoroptic temperature probe was positioned at the center or edge of the electrode-tissue interface.

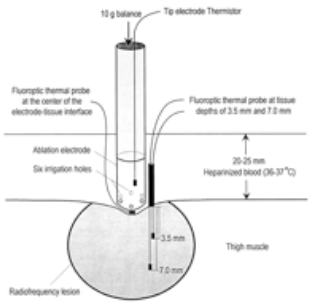

View larger version (65K):
In this window
In a new window

Figure 2. Schematic of the 7F ablation catheter in the canine thigh muscle preparation. The catheter has a central lumen (not shown) and a 5-mm tip electrode with six 0.4-mm-diameter irrigation holes located around the electrode 1.0 mm from the tip. The electrode has an internal thermistor 2.5 mm from the tip. The catheter was positioned perpendicular to the thigh muscle and held with a constant contact weight of 10 g. The electrode tip was irrigated through the central lumen with heparinized saline at 20 mL/min during radiofrequency applications of constant voltage (CV) with saline irrigation. Two fluoroptic thermal probes were inserted at 3.5 and 7.0 mm deep into the tissue adjacent to the electrode to record tissue temperature. An additional fluoroptic thermal probe was positioned at the center or edge (not shown) of the electrode-tissue interface in 33 of 75 applications for the CV irrigation group.

The ablation electrode was irrigated through the catheter lumen with room temperature (20°C to 22°C) heparinized (2 U/mL) normal saline at 20 mL/min using a Harvard infusion pump (model 55-2083). The saline irrigation was started 3 to 5 seconds before the onset of the application of radiofrequency current and was maintained until 5 seconds after the completion of the application of energy. Radiofrequency current (550 to 650 kHz) was produced by a constant voltage (CV) generator (American Cardiac Ablation Co, model LIZ-88) and was delivered between the catheter tip electrode and an adhesive electrosurgical dispersive pad applied to the shaved skin of the abdominal wall. During each application of radiofrequency current, the RMS voltage and current, the impedance, and the temperatures measured from the thermistor in the ablation electrode and the tissue probes were continuously monitored and recorded on optical disk (Bard LabSystem).

Ablation Protocol

Five to eight applications of radiofrequency current were delivered to separate sites on the right thigh muscle. The skin incision was closed, the dog was turned onto its right side, and five to eight applications of radiofrequency current were delivered at separate sites on the left thigh muscle.

Radiofrequency current was delivered using three approaches: (1) The constant voltage (CV) group received high CV (66 V) without irrigation (n=31 applications); (2) the temperature-control group received variable voltage (20 to 66 V) to maintain tip-electrode temperature at 80°C to 90°C without irrigation (n=39 applications); and (3) the CV irrigation group received high CV (66 V) with saline irrigation (n=75 applications). In all three groups, radiofrequency current was applied for 60 seconds but was terminated immediately in the event of an impedance rise of ≥10 Ω. The ablation tip electrode was examined for coagulum after each application of radiofrequency energy. Before the next application, the tip-electrode surface and irrigation holes were cleaned by use of a gauze pad soaked in heparinized saline and a 0.3-mm-diameter drill bit.

After Ablation

Two hours after the ablation procedure was completed, 2% triphenyl tetrazolium chloride (30 mL IV) was administered. This dye stains intracellular dehydrogenase, which distinguishes viable and necrotic tissue. The dogs were killed and their thigh muscles were excised, fixed in a 10% formalin solution, and sectioned.

Measurements of Lesion Size

The maximal depth (A), maximal diameter (B), depth at the maximal diameter (C), and lesion surface diameter (D) were measured. The lesion volume (V_L) was calculated with the following formula for an oblate ellipsoid by subtracting the volume of the ellipsoid extending above the surface of the muscle ("missing cap").[35]

$$V_L=[0.75\pi(B/2)^2(A-C)]-[0.25\pi(D/2)^2(A-2C)]$$

Statistical Analysis

The electrical parameters of radiofrequency delivery, tip-electrode temperature, tissue temperatures at 3.5- and 7.0-mm depths, and lesion dimensions were compared among the three groups by ANOVA. Any significant differences were measured by Scheffé's method for pairwise comparisons. The values are expressed as mean±SD. The significance of the relations between lesion size and total radiofrequency energy, tip-electrode temperature, and tissue temperature was assessed by linear-regression analysis. A value of $P<.05$ was considered statistically significant.

Results

Radiofrequency Energy Parameters During Ablation

The mean voltage, current, impedance, power, duration, and energy of the applications of radiofrequency current are compared among the three groups in Fig 3. The impedance was not significantly different for the three groups (mean, 84 to 86 Ω). In the CV group, application of 66 V resulted in a mean current of 0.79±0.06 A and a mean power of 52.3±3.8 W. An impedance rise >10 Ω occurred in all 31 CV group applications at a mean of 11.6±4.8 seconds, which prematurely terminated each application of radiofrequency current. All the impedance rises were associated with a film of coagulum on the electrode. The impedance rise was gradual in 28 CV group applications and was abrupt and associated with an audible pop in the remaining 3 applications. The short duration of the applications resulted in a mean energy of only 605±260 J.

Figure 3. Bar graphs showing electrical parameters during radiofrequency applications in the constant voltage (CV), temperature-control (TC), and CV with saline irrigation (CV-Irrig) groups. Voltage (A), current (B), and power (D)

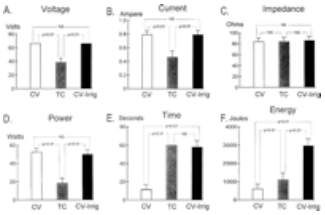

View larger version (32K):
In this window
In a new window

were significantly lower for the TC group than for the CV group or CV-Irrig group. There was no significant difference in impedance among the three groups (C). Time of radiofrequency current application (E) was significantly shorter in the CV group than in the TC and CV-Irrig groups. Total radiofrequency energy delivered (F) was the lowest in the CV group, intermediate in the TC group, and highest in the CV-Irrig group.

In the temperature-control group applications, the radiofrequency voltage was regulated to maintain a tip-electrode temperature of 80°C to 90°C. This prevented an impedance rise, and all 39 applications were delivered for the full 60 seconds. Although the initial voltage was relatively high (48.2±4.1 V), the steady state voltage was only 38.4±6.1 V; this voltage was obtained 10 to 15 seconds after the onset of the application. The mean current at steady state was 0.46±0.09 A and resulted in a mean power of only 18.3±6.4 W. The mean energy for the temperature-control applications was 1098±380 J.

In the CV irrigation (saline irrigation) group, 69 of 75 radiofrequency applications were maintained for the full 60 seconds without an impedance rise. Six of 75 applications (8%) resulted in a small (≈10 Ω), abrupt impedance rise at 30 to 51 seconds. All 6 impedance rises were accompanied by an audible pop, and none of the 6 were associated with coagulum formation on the electrode. The mean current for the CV irrigation applications was 0.77±0.07 A, which resulted in a mean power of 50.6±4.7 W. This power was not significantly different from that in the CV group, but the sustained duration of the applications resulted in a mean energy of 2934±389 J, which was markedly greater than the energy in the CV and temperature-control groups.

Tip-Electrode Temperature and Tissue Temperatures

The peak tip-electrode and peak tissue temperatures at depths of 3.5 and 7.0 mm are compared for the three groups in Fig 4. In the CV group, the tip-electrode temperature reached ≈100°C (mean, 98.8±2.1°C) for all 31 applications of radiofrequency current (Fig 4A). A >10-Ω impedance rise occurred in all applications at an electrode temperature of 95°C to 105°C (Fig 5). Due to the early rise in impedance, the peak tissue temperature at 3.5 mm was 62.1±15.1°C and the peak temperature at 7 mm was only 40.3±5.3°C (Fig 4B and 4C). A temperature of ≥50°C, which was thought to correspond to the temperature required to produce necrosis,[28 29] was reached in 23 of 31 CV applications at 3.5 mm but in only 2 of 31 applications at 7 mm.

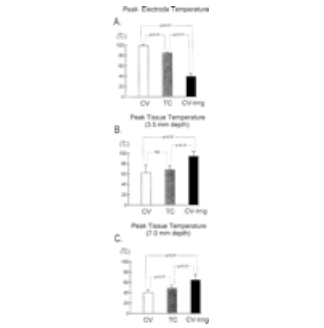

View larger version (17K):
In this window
In a new window

Figure 4. Bar graphs showing peak electrode temperature and tissue temperatures at 3.5- and 7.0-mm depths during radiofrequency applications in the constant voltage (CV), temperature-control (TC), and CV irrigation (CV-Irrig) groups. In the CV-Irrig group, the peak electrode temperature was significantly lower and the tissue temperature at each depth was significantly greater than in the other groups.

Figure 5. Diagram showing a constant high-voltage (66-V) application of radiofrequency current without irrigation. Electrode temperature increased rapidly and was associated with a progressive decrease in impedance from 85 to 80 Ω and an increase in current from 0.78 to 0.82 A (power, 54 W). At 8 seconds, the electrode temperature reached 97°C, which was associated with an impedance rise (from 80 to 94 Ω) and a decrease in current (from 0.82 to 0.70 A). The peak tissue temperatures during application of radiofrequency energy at depths of 3.5 and 7.0 mm were only 54°C and 38°C, respectively.

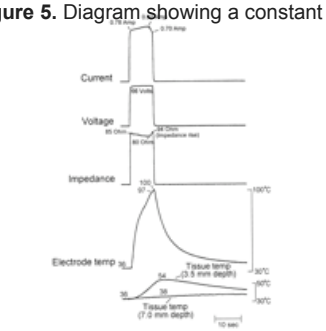

View larger version (18K):
In this window
In a new window

For the temperature-control group, the tip-electrode temperature was maintained at 80°C to 90°C (mean, 84.5±1.4°C; Figs 4A and 6). The peak temperature at 3.5 mm was 67.9±7.5°C. Although this value was not statistically greater than the value for the CV group, all 39 applications for the temperature-control group

resulted in a tissue temperature of ≥50°C at 3.5 mm. The peak temperature at 7 mm was 48.3±4.8°C for the temperature-control group applications (or significantly greater than CV group applications), with a temperature ≥50°C in 11 of the 39 applications.

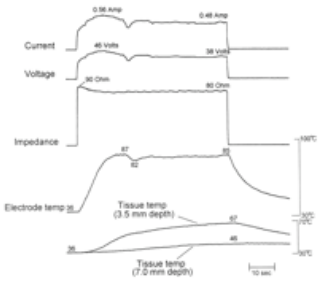

View larger version (19K):
In this window
In a new window

Figure 6. Diagram showing application of radiofrequency current for the temperature-control group. Voltage was adjusted to achieve and maintain an electrode temperature (temp) of 80°C to 90°C. Voltage was initially increased to 46 V (power, 26 W) and then decreased to 38 V (power, 18 W) to maintain an electrode temperature of 85°C. Impedance decreased rapidly from 90 to 80 Ω as electrode temperature increased from 36°C to 87°C, then remained essentially constant with the constant electrode temperature. The tissue temperature at depths of 3.5 and 7.0 mm increased gradually during the application of radiofrequency energy and reached 67°C and 46°C, respectively.

For the CV irrigation group applications, the peak tip-electrode temperature ranged from 30°C to 48°C (mean, 38.4±5.1°C; Figs 4A↑ and 7↓). The ability to sustain the radiofrequency current at high power for 60 seconds resulted in a peak temperature of 94.7±9.1°C at 3.5 mm and of 65.1±9.7°C at 7.0 mm. These tissue temperatures were significantly greater than in applications for the CV and temperature-control groups (Fig 4↑). The temperature exceeded 50°C at both the shallow and deep sites (3.5 and 7.0 mm) in all 75 applications.

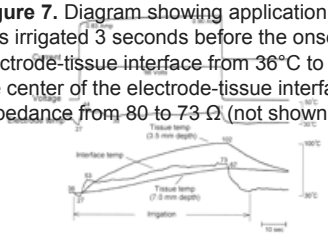

View larger version (18K):
In this window
In a new window

Figure 7. Diagram showing application of radiofrequency current at constant high voltage (66 V) with saline irrigation (constant voltage irrigation group). Saline was irrigated 3 seconds before the onset of radiofrequency application; this decreased the temperature of the tip electrode and of the region at the center of the electrode-tissue interface from 36°C to 27°C. The tip-electrode temperature was 38°C to 44°C throughout the radiofrequency application. The temperature at the center of the electrode-tissue interface increased quickly to 53°C and then increased gradually to 73°C. This increase was associated with a decrease in impedance from 80 to 73 Ω (not shown) and an increase in current from 0.83 to 0.90 A (power increase, 55 to 59 W). The sustained high power progressively increased the tissue temperatures at 3.5- and 7.0-mm depths to 102°C and 67°C, respectively.

An additional optical temperature probe was positioned at the center of the electrode-tissue interface in 18 CV irrigation group radiofrequency current applications and at the edge of the electrode-tissue interface in 15 CV irrigation group applications (Fig 2↑). The electrode-tissue interface temperature did not reach 100°C in any of these 33 applications. The peak temperature at the center of the electrode-tissue interface was 69.4±5.7°C, and the peak temperature at the edge of the electrode-tissue interface was 51.1±2.9°C. At 3.5 mm, these interface temperatures exceeded the electrode temperature but were less than the tissue temperature at 3.5 mm (Fig 7↑). In 4 applications, the electrode-tissue interface temperature was lower than the tissue temperature at 7 mm.

In all three groups, the tissue temperature at the 3.5- and 7.0-mm depths was still increasing at the end of every radiofrequency application, including those applications that extended for the full 60 seconds (Figs 6↑ and 7↑).

Lesion Geometry

All lesions were sharply demarcated and ellipsoid. The size and depth of the center of the ellipsoids were different for the three groups (Figs 8↓ and 9↓). In the CV group, the center of the ellipsoid was located at the surface of the tissue, such that the maximal diameter of the lesion was the same as the surface diameter. In the temperature-control group, the center of the ellipsoid (the maximal lesion diameter) was displaced at 1.2±0.5 mm below the surface. The lesion surface diameter was 10.3±0.9 mm, and the largest diameter was 11.3±0.9 mm. In the CV irrigation group, almost all the ellipsoid was below the surface, such that the maximal lesion diameter was located 4.1±0.7 mm from the surface. The lesion surface had a significantly smaller diameter than the maximal diameter (10.1±1.3 versus 14.3±1.5 mm, $P<.01$). The lesion depth, maximal diameter, depth at maximal diameter, and volume were significantly greater in lesions in the CV irrigation group than those in the temperature-control group and were significantly greater in lesions in the temperature-control group than those in the CV group (Fig 9↓). Interestingly, the lesion surface diameter was not significantly different among the three groups.

THIS FIGURE IS
CURRENTLY UNAVAILABLE

We apologize for
any inconvenience.

View larger version (0K):
In this window

Figure 8. Photograph showing a representative lesion for each of three groups studied. All three lesions were ellipsoid. In the lesion from the constant voltage (CV) group (left), the center of the ellipsoid was located at the surface of the tissue. In the lesion for the temperature-control group (center), the center of the ellipsoid was displaced slightly below the surface (arrows). This lesion is deeper and larger than the CV group lesion. In the lesion for the constant voltage with (saline) irrigation group (right), the maximal lesion diameter was deeper within the tissue (arrows) and almost all the ellipsoid was below the surface. This lesion was deeper and wider than the CV and temperature-control group lesions and had a circumscribed pale central area below the surface, possibly indicating the location of the highest tissue temperature. Note that lesion surface diameter was similar for the three lesions.

In a new window

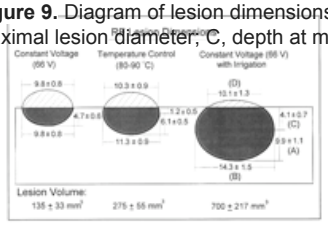

Figure 9. Diagram of lesion dimensions for the three groups studied. Values are expressed in millimeters (mean±SD). A indicates maximal lesion depth; B, maximal lesion diameter; C, depth at maximal lesion diameter; and D, lesion surface diameter. Lesion volume was calculated by use of the formula for an oblate ellipsoid by subtracting the volume of the "missing cap" (hatched area) (see text).

View larger version (46K):
In this window
In a new window

A shallow crater (1 to 2 mm in depth and 1 to 3 mm in diameter) was found on the surface of two lesions from the CV group and three from the CV irrigation group. A small, abrupt impedance rise associated with an audible pop occurred during each of the 5 radiofrequency applications, producing these lesions. Four other applications of radiofrequency current (one in the CV group and three in the CV irrigation group, Fig 10⬥) resulted in an abrupt impedance rise with an audible pop, but neither a crater nor a tear was found when these four lesions were examined.

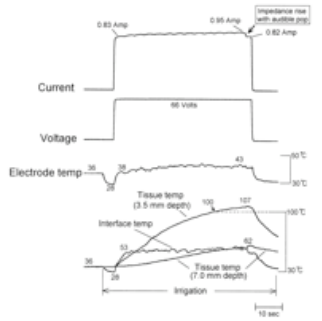

Figure 10. Diagram showing radiofrequency application for the constant voltage with (saline) irrigation group, associated with an abrupt impedance rise accompanied by an audible pop. The electrode-tissue interface temperature increased slowly to 62°C, which was associated with a progressive decrease in impedance (not shown) and manifested by an increase in current from 0.83 to 0.95 A. An abrupt impedance rise from 69 to 80 Ω occurred, was accompanied by an audible pop, and was reflected by an abrupt decrease in current from 0.95 to 0.82 A (arrow). Since the electrode-tissue interface temperature did not approach 100°C, the rise in impedance probably resulted from the release of steam from below the surface, where the tissue temperature reached 107°C.

View larger version (23K):
In this window
In a new window

Relation Between Tissue Temperatures and Lesion Dimensions

The relations between each of the measurements of lesion size and total radiofrequency energy, tip-electrode temperature, and tissue temperatures at depths of 3.5 and 7.0 mm were examined. Lesion depth correlated best with tissue temperature measured at 7 mm (Fig 11A⬥). Linear regression for that relation predicts that necrosis extending to 7 mm would correspond to a temperature of 48.4°C at that depth. The largest lesion diameter corresponded best with tissue temperature recorded at 3.5 mm (Fig 11B⬥). In CV irrigation group applications, there was no correlation between either the depth or the maximal diameter of the lesion and either the electrode temperature or the electrode-tissue interface temperature.

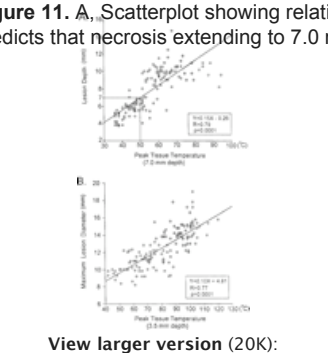

Figure 11. A, Scatterplot showing relation between lesion depth and peak tissue temperature at 7.0 mm deep for all 145 lesions. Linear-regression analysis predicts that necrosis extending to 7.0 mm corresponds to a temperature of 48.4°C at that depth. B, Scatterplot showing relation between maximal lesion diameter and peak tissue temperature at 3.5 mm deep for all 145 lesions.

View larger version (20K):
In this window
In a new window

Discussion

The application of radiofrequency energy at 66 V without irrigation (CV group) resulted in a quick impedance rise at a mean of 11.6±4.8 seconds. The short

application time resulted in the smallest lesions among the three groups. In the temperature-control group, adjusting the voltage to maintain the tip-electrode temperature at 80°C to 90°C prevented an impedance rise, which allowed the sustained application of radiofrequency energy. However, to prevent the electrode temperature from approaching 100°C, the voltage had to be reduced to a relatively low level (38.4±6.1 V; power, 18.3±6.4 W), which limited lesion size and depth. In the CV irrigation group, saline irrigation prevented the tip-electrode temperature and the electrode-tissue interface temperature from reaching 100°C, which allowed the sustained application of radiofrequency current at higher voltage (66±0 V; power, 50.6±4.7 W). This sustained application at high power resulted in a significant increase in lesion size and depth. The mean lesion depth for the CV irrigation group was 9.9±1.1 mm, compared with 6.1±0.5 mm for the temperature-control group and 4.7±0.6 mm for the CV group.

In previous studies, lesion size approached maximum after application of radiofrequency for ≈20 to 60 seconds.[21] [28] In the present study, the tissue temperatures at depths of 3.5 and 7.0 mm continued to increase at the end of each radiofrequency application in all three groups (Figs 5 through 7♠♠♠ and 10). For the 7.0-mm depth in the temperature-control group, at the end of 60 seconds, the temperature was increasing at a slow rate (Fig 6♠), which suggests that extending the radiofrequency application beyond 60 seconds probably would not have increased lesion depth substantially. In contrast, at 60 seconds in the CV irrigation group at 7.0 mm, the temperature continued to increase at a steep rate (Figs 7♠ and 10♠), which suggests that longer applications of radiofrequency current with saline irrigation may result in significantly deeper lesions.

Although the electrode temperature and electrode-tissue interface temperature did not reach 100°C for any of the applications in the CV irrigation group, an impedance rise occurred in 6 of 75 applications after 30 to 51 seconds (Fig 10♠). All 6 of the impedance rises were small, abrupt, and associated with an audible pop. There was no coagulum on the electrode. A small crater was found on the surface of 3 of these 6 lesions. These observations suggest that the impedance rise associated with radiofrequency applications in the CV irrigation group may have resulted from a sudden release of steam from below the surface of the lesion rather than from boiling at the electrode-tissue interface.[36] The tissue temperature at a depth of 3.5 mm immediately preceding the abrupt impedance rise with an audible pop was 97°C to 120°C (Fig 10♠), which is consistent with superheating of the tissue and steam formation. Prevention of tissue superheating during radiofrequency application with irrigation would require the measurement of tissue temperature, since the electrode-tissue interface temperature does not reflect the temperature of the underlying tissue.

For 28 of 31 radiofrequency applications in the CV group, the impedance rise was gradual and was associated with an electrode temperature of ≈100°C and coagulum formation on the electrode (Fig 5♠). These observations are consistent with the findings of earlier investigators that suggested that, in the absence of active electrode cooling, the impedance rise results from boiling at the electrode-tissue interface.[22] [23] [24]

Tissue temperatures during radiofrequency ablation with saline irrigation (CV irrigation group) were significantly higher than in the CV and temperature-control groups (without irrigation), even though the tip-electrode temperature was lowest, ranging from 30°C to 48°C (Figs 4 through 7♠♠♠♠). The electrode-tissue interface temperature during radiofrequency ablation with irrigation was higher than the temperature recorded with the thermistor positioned in the electrode. However, the electrode-tissue interface temperature was always lower than the tissue temperature measured at 3.5 mm and was occasionally lower than the tissue temperature at 7.0 mm. These data suggest that the temperature at the electrode-tissue interface results from the competing effects of heating from the underlying tissue and convective cooling by irrigation. The higher tissue temperature than electrode-tissue interface temperature indicates that resistive (electrical) heating extended several millimeters below the surface rather than just extending along a thin layer of myocardium surrounding the electrode. Previous studies have shown that the size of radiofrequency lesions correlates well with tip-electrode temperature.[27] [28] [29] This relation is significantly altered when saline irrigation is used to cool the ablation electrode. With electrode cooling, neither electrode temperature nor electrode-tissue interface temperature can be used to predict lesion size.

The differences in lesion geometry among the three groups may be explained by differences in (1) the rate at which heat is generated within the tissue, (2) the duration of time in which heat is generated, and (3) the rate of heat removal from the tissue surface by convective cooling from the blood and saline irrigation. In the CV group, heat was generated quickly for a short period, preventing significant convective cooling by the blood. This resulted in a shallow lesion, with maximal diameter at the surface. In the temperature-control group, the rate of heat generation was slowed by the reduction in radiofrequency power, which allowed some convective cooling by the blood. The longer application time resulted in a deeper and larger lesion, with the maximal diameter located slightly below the surface owing to surface cooling by the blood. In the CV irrigation group, the rate of heat generation was high and the application time was long. However, the surface convective cooling was greatly increased by the saline irrigation. This resulted in a deeper and larger lesion, with the maximal diameter located farther from the surface, at a mean depth of 4.1 mm. The size of the lesion surface was not significantly larger than in the CV and temperature-control groups, despite the greater depth and diameter of the intramural lesion. The small size of the surface lesion may be clinically beneficial for reducing the risk of mural thrombus and thromboembolic complications.

Lesion depth correlated closely with peak tissue temperature at a depth of 7.0 mm. Linear-regression analysis suggests that, in this canine thigh muscle preparation, a lesion will extend to 7.0 mm when the temperature at that depth reaches 48.4°C (Fig 11A♠). This temperature correlates closely with the 48°C to 50°C temperature that was shown to produce necrosis in myocardium in previous studies.[28] [29] Maximal lesion diameter correlated well with peak tissue temperature at a depth of 3.5 mm (Fig 11B♠).

Study Limitations

This study was performed in a canine thigh muscle preparation instead of the endocardium of a beating heart to control tip-electrode contact pressure and to allow measurement of temperatures at various tissue depths beneath the electrode. The flat surface of the thigh muscle also allows accurate determination of lesion size and geometry. In contrast, delivering radiofrequency current to the trabeculated endocardium often results in an irregular lesion shape and greater variation in lesion size than was found in this study.

Because the intramural blood flow may be less in the resting thigh muscle than in the myocardium, the thigh muscle may provide less heat sink and therefore may result in greater lesion size. However, a previous study[28] has suggested that the tissue temperature profile during radiofrequency ablation may be independent of intramyocardial perfusion. In addition, in the present study, the size of the lesions in the CV and temperature-control groups is similar to the lesions described in other studies of the canine heart.[21] [32] [37]

Clinical Implications

The results of this study indicate that radiofrequency current can be delivered for a prolonged period at higher power by cooling the ablation electrode with saline

irrigation. The higher power produces a wider, deeper lesion without increasing the diameter of the endocardial surface of the lesion. The use of an irrigated electrode may allow the ablation of arrhythmogenic tissue farther from the endocardium (deeper) and may significantly improve the efficacy of ablation in ventricular tachycardia associated with structural heart disease and some difficult-to-reach locations of accessory pathways.

Acknowledgments

This study was supported by grants from the NIH (R01-HL-39670) and from the Oklahoma Center for the Advancement of Science and Technology (HRI-104). The authors thank Dr Fred H.M. Wittkampf for his thoughtful review of the manuscript and helpful suggestions.

Received August 16, 1994; revision received November 7, 1994; accepted November 20, 1994.

References

1. Jackman WM, Wang X, Friday KJ, Roman CA, Moulton KP, Beckman KJ, McClelland JH, Twidale N, Hazlitt HA, Prior MI, Margolis PD, Calame JD, Overholt ED, Lazzara R. Catheter ablation of accessory AV pathways (Wolff-Parkinson-White syndrome) by radiofrequency current. *N Engl J Med.* 1991;324:1605-1611. [Medline] [Order article via Infotrieve]

2. Calkins H, Sousa J, El-Atassi R, Rosenheck S, de Buitleir M, Kou WH, Kadish AH, Langberg JJ, Morady F. Diagnosis and cure of the Wolff-Parkinson-White syndrome or paroxysmal supraventricular tachycardias during a single electrophyiological test. *N Engl J Med.* 1991;324:1612-1618. [Medline] [Order article via Infotrieve]

3. Kuck KH, Schluter M, Geiger M, Siebels J, Duckeck W. Radiofrequency current catheter ablation of accessory atrioventricular pathways. *Lancet.* 1991;337:1557-1561. [Medline] [Order article via Infotrieve]

4. Lesh MD, Van Hare GF, Schamp DJ, Chien W, Lee M, Griffin JC, Langberg JJ, Cohen TJ, Lurie KG, Scheinman MM. Curative percutaneous catheter ablation using radiofrequency energy for accessory pathways in all locations: results in 100 consecutive patients. *J Am Coll Cardiol.* 1992;19:1303-1309. [Abstract]

5. Lee MA, Morady F, Kadish A, Schamp DJ, Chin MC, Scheinman MM, Griffin JC, Lesh MD, Pederson D, Goldberger J, Calkins H, de Buitleir M, Kou WH, Rosenheck S, Sousa J, Langberg JJ. Catheter modification of the atrioventricular junction with radiofrequency energy for control of atrioventricular nodal reentry tachycardia. *Circulation.* 1991;83:827-835. [Abstract/Free Full Text]

6. Jackman WM, Beckman KJ, McClelland JH, Wang X, Friday KJ, Roman CA, Moulton KP, Twidale N, Hazlitt HA, Prior MI, Oren J, Overholt ED, Lazzara R. Treatment of supraventricular tachycardia due to atrioventricular nodal reentry by radiofrequency catheter ablation of slow-pathway conduction. *N Engl J Med.* 1992;327:313-318.[Medline] [Order article via Infotrieve]

7. Kay GN, Epstein AE, Dailey SD, Plumb VJ. Selective radiofrequency ablation of the slow pathway for the treatment of atrioventricular nodal reentrant tachycardia: evidence for involvement of perinodal myocardium within the reentrant circuit. *Circulation.* 1992;85:1675-1688. [Abstract/Free Full Text]

8. Jazayeri MR, Hempe SL, Sra JS, Dhala AA, Blanck Z, Deshpande SS, Avitall B, Krum DP, Gilbert CJ, Akhtar M. Selective transcatheter ablation of the fast and slow pathways using radiofrequency energy in patients with atrioventricular nodal reentrant tachycardia. *Circulation.* 1992;85:1318-1328. [Abstract/Free Full Text]

9. Klein LS, Shih H, Hackett FK, Zipes DP, Miles WM. Radiofrequency catheter ablation of ventricular tachycardia in patients without structural heart disease. *Circulation.* 1992;85:1666-1674. [Abstract/Free Full Text]

10. Nakagawa H, Beckman KJ, McClelland JH, Wang X, Arruda M, Santoro I, Hazlitt A, Abdalla I, Singh A, Gossinger H, Sweidan R, Hirao K, Widman L, Pitha JV, Lazzara R, Jackman WM. Radiofrequency catheter ablation of idiopathic left ventricular tachycardia guided by a Purkinje potential. *Circulation.* 1993;88:2607-2617. [Abstract/Free Full Text]

11. Haissaguerre M, Gaita F, Fischer B, Egloff P, Lemetayer P, Warin JF. Radiofrequency catheter ablation of left lateral accessory pathways via the coronary sinus. *Circulation.* 1992;86:1464-1468. [Abstract/Free Full Text]

12. Wang X, McClelland J, Beckman K, Oren J, Calame J, Roman C, Santro I, Arruda M, Nakagawa H, Hirao K, Lazzara R, Jackman W. Left free-wall accessory pathways which require ablation from the coronary sinus: unique coronary sinus electrogram pattern. *Circulation.* 1992;86:I-581. Abstract.

13. Arruda MS, Beckman KJ, McClelland JH, Wang X, Nakagawa H, Widman LE, Hazlitt HA, Lazzara R, Jackman WM. Coronary sinus anatomy and anomalies in patients with posteroseptal accessory pathway requiring ablation within a venous branch of the coronary sinus. *J Am Coll Cardiol.* 1994;224A. Abstract.

14. Kuck KH, Schluter M, Geiger M, Siebels J. Successful catheter ablation of human ventricular tachycardia with radiofrequency current guided by an endocardial map of the area of slow conduction. *PACE Pacing Clin Electrophysiol.* 1991;14:1060-1071. [Medline] [Order article via Infotrieve]

15. Fitzgerald DM, Friday KJ, Yeung Lai Wah JA, Lazzara R, Jackman WM. Myocardial regions of slow conduction participating in the reentrant circuit of multiple ventricular tachycardias: report on ten patients. *J Cardiovasc Electrophysiol.* 1991;2:193-206.

16. Morady F, Harvey M, Kalbfleisch SJ, El-Atassi R, Calkins H, Langberg JJ. Radiofrequency catheter ablation of ventricular tachycardia in patients with coronary artery disease. *Circulation.* 1993;87:363-372. [Abstract/Free Full Text]

17. Kim YH, Sosa-Suarez G, Trouton TG, O'Nunain SS, Osswald S, McGovern BA, Ruskin JN, Garan H. Treatment of ventricular tachycardia by transcatheter radiofrequency ablation in patients with ischemic heart disease. *Circulation.* 1994;89:1094-1102.[Abstract/Free Full Text]

18. Littmann L, Svenson RH, Gallagher JJ, Selle JG, Zimmern SH, Fedor JM, Colavita PG. Functional role of the epicardium in postinfarction ventricular tachycardia: observations derived from computerized epicardial activation mapping, entrainment, and epicardial laser photoablation. *Circulation.* 1991;83:1577-1591. [Abstract/Free Full Text]

19. Downar E, Kimber S, Harris L, Mickleborough L, Sevaptsidis E, Masse S, Chen TCK, Genga A. Endocardial mapping of ventricular tachycardia in the intact human heart, II: evidence for multiuse reentry in a functional sheet of surviving myocardium. *J Am Coll Cardiol.* 1992;20:869-878. [Abstract]

20. Hoyt RH, Huang SK, Marcus FI, Roger S. Factors influencing trans-catheter radiofrequency ablation of the myocardium. *J Appl Cardiol.* 1986;1:469-486.

21. Wittkampf FHM, Hauer RNW, Robles de Medina EO. Control of radiofrequency lesion size by power regulation. *Circulation.* 1989;80:962-968. [Abstract/Free Full Text]

22. Ring ME, Huang SKS, Gorman G, Graham AR. Determinants of impedance rise during catheter ablation of bovine myocardium with radiofrequency energy. *PACE Pacing Clin Electrophysiol.* 1989;12:170-176. [Medline] [Order article via Infotrieve]

23. Haines DE, Verow AF. Observation on electrode-tissue interface temperature and effect on electrical impedance during radiofrequency ablation of ventricular myocardium. *Circulation.* 1990;82:1034-1038. [Abstract/Free Full Text]

24. Langberg JJ, Calkins H, El-Atassi R, Borganelli M, Leon A, Kalbfleisch SJ, Morady F. Temperature monitoring during radiofrequency catheter ablation of accessory pathways. *Circulation.* 1992;86:1469-1474. [Abstract/Free Full Text]

25. Organ LW. Electrophysiologic principles of radiofrequency lesion making. *Appl Neurophysiol.* 1976;39:60-76.

26. Erez A, Smitzer A. Controlled destruction and temperature distributions in biological tissues subjected to monoactive electrocoagulation. *J Biomech Eng.* 1980;102:42-49. [Medline] [Order article via Infotrieve]

27. Haverkamp W, Hindricks G, Gulker H, Rissel U, Pfennings W, Borggrefe M, Breithardt G. Coagulation of ventricular myocardium using radiofrequency alternating current: biophysical aspects and experimental findings. *PACE Pacing Clin Electrophysiol.* 1989;12:187-195. [Medline] [Order article via Infotrieve]

28. Haines DE, Watson DD. Tissue heating during radiofrequency catheter ablation: a thermodynamic model and observations in isolated perfused and superfused canine right ventricular free wall. *PACE Pacing Clin Electrophysiol.* 1989;12:962-976. [Medline] [Order article via Infotrieve]

29. Haines DE, Watson DD, Verow AF. Electrode radius predicts lesion radius during radiofrequency energy heating: validation of a proposed thermodynamic model. *Circ Res.* 1990;67:124-129. [Abstract/Free Full Text]

30. Kalbfleisch SJ, Langberg JJ. Catheter ablation with radiofrequency energy: biophysical aspects and clinical applications. *J Cardiovasc Electrophysiol.* 1992;3:173-186.

31. Haines DE. The biophysics of radiofrequency catheter ablation in the heart: the importance of temperature monitoring. *PACE Pacing Clin Electrophysiol.* 1993;16:586-591. [Medline] [Order article via Infotrieve]

32. Langberg JJ, Gallagher M, Strickberger SA, Amirana O. Temperature-guided radiofrequency catheter ablation with very large distal electrode. *Circulation.* 1993;88:245-249. [Abstract/Free Full Text]

33. Wittkampf FH, Hauer RN, Robles de Medina EO. Radiofrequency ablation with a cooled porous electrode catheter. *J Am Coll Cardiol.* 1988;11:17. Abstract.

34. Huang SKS, Cuenoud H, Tan-de-Guzman W. Increase in lesion size and decrease in impedance rise with a saline infusion electrode catheter for radiofrequency catheter ablation. *Circulation.* 1989;80:II-324. Abstract.

35. Spiege MR. *Mathematical Handbook of Formulas and Tables; Schaum's Outline Series*. New York, NY: McGraw Hill; 1968:7-10.

36. Avitall B, Morgan M, Hare J, Khan M, Lessila C. Intracardiac explosions during radiofrequency ablation: histopathology in the acute and chronic dog model. *Circulation.* 1992;86:I-191. Abstract.

37. Langberg JJ, Lee MA, Chin MC, Rosenqvist M. Radiofrequency catheter ablation: the effect of electrode size on lesion volume in vivo. *PACE Pacing Clin Electrophysiol.* 1990;13:1242-1248.[Medline] [Order article via Infotrieve]

Articles citing this article

Percutaneous Radiofrequency Septal Reduction for Hypertrophic Obstructive Cardiomyopathy in Children
J Am Coll Cardiol. 2011;58:2501-2510,
Abstract| **Full Text**| **PDF**

Outcomes of Cardiac Perforation Complicating Catheter Ablation of Ventricular Arrhythmias
Circ Arrhythm Electrophysiol. 2011;4:660-666,
Abstract| **Full Text**| **PDF**

Findings and outcome of fluoroscopic visualization of the oesophageal course during catheter ablation of atrial fibrillation
Europace. 2011;13:796-802,
Abstract | **Full Text** | **PDF**

Assessment of Catheter Tip Contact Force Resulting in Cardiac Perforation in Swine Atria Using Force Sensing Technology
Circ Arrhythm Electrophysiol. 2011;4:218-224,
Abstract | **Full Text** | **PDF**

Assessment of Radiofrequency Ablation Lesions by CMR Imaging After Ablation of Idiopathic Ventricular Arrhythmias
J Am Coll Cardiol Img. 2010;3:278-285,
Abstract | **Full Text** | **PDF**

Updated Worldwide Survey on the Methods, Efficacy, and Safety of Catheter Ablation for Human Atrial Fibrillation
Circ Arrhythm Electrophysiol. 2010;3:32-38,
Abstract | **Full Text** | **PDF**

Efficacy of a cooled bipolar epicardial radiofrequency ablation probe for creating transmural myocardial lesions
J. Thorac. Cardiovasc. Surg.. 2010;139:453-458,
Abstract | **Full Text** | **PDF**

EHRA/HRS Expert Consensus on Catheter Ablation of Ventricular Arrhythmias: Developed in a partnership with the European Heart Rhythm Association (EHRA), a Registered Branch of the European Society of Cardiology (ESC), and the Heart Rhythm Society (HRS); in collaboration with the American College of Cardiology (ACC) and the American Heart Association (AHA)
Europace. 2009;11:771-817,
Full Text | **PDF**

In vitro comparison of platinum-iridium and gold tip electrodes: lesion depth in 4 mm, 8 mm, and irrigated-tip radiofrequency ablation catheters
Europace. 2009;11:565-570,
Abstract | **Full Text** | **PDF**

Mitral valve surgery plus concomitant atrial fibrillation ablation is superior to mitral valve surgery alone with an intensive rhythm control strategy
Eur. J. Cardiothorac. Surg.. 2009;35:641-650,
Abstract | **Full Text** | **PDF**

Cooled ablation reduces pulmonary vein isolation time: results of a prospective randomised trial
Heart. 2009;95:203-209,
Abstract | **Full Text** | **PDF**

Irrigated Radiofrequency Catheter Ablation Guided by Electroanatomic Mapping for Recurrent Ventricular Tachycardia After Myocardial Infarction: The Multicenter Thermocool Ventricular Tachycardia Ablation Trial
Circulation. 2008;118:2773-2782,
Abstract | **Full Text** | **PDF**

Novel Contact Force Sensor Incorporated in Irrigated Radiofrequency Ablation Catheter Predicts Lesion Size and Incidence of Steam Pop and Thrombus
Circ Arrhythm Electrophysiol. 2008;1:354-362,
Abstract | **Full Text** | **PDF**

Ventricular Tachycardia Ablation: Evolution of Patients and Procedures Over 8 Years
Circ Arrhythm Electrophysiol. 2008;1:153-161,
Abstract | **Full Text** | **PDF**

Can We Improve Upon Human Performance in the Electrophysiology Laboratory?
J Am Coll Cardiol. 2008;51:2412-2413,
Full Text | **PDF**

Permanent Chronic Atrial Fibrillation: Is Pulmonary Vein Isolation Alone Enough?
Ann. Thorac. Surg.. 2007;84:1151-1157,
Abstract | **Full Text** | **PDF**

Pulmonary Vein Antral Isolation Using an Open Irrigation Ablation Catheter for the Treatment of Atrial Fibrillation: A Randomized Pilot Study
J Am Coll Cardiol. 2007;49:1634-1641,
Abstract | **Full Text** | **PDF**

Radiofrequency energy delivery for pulmonary vein isolation: is less more?
Europace. 2006;8:966-967,
Full Text | **PDF**

The effectiveness of a high output/short duration radiofrequency current application technique in segmental pulmonary vein isolation for atrial fibrillation.
Europace. 2006;8:962-965,
Abstract | **Full Text** | **PDF**

Combined atrial septal defect surgical closure and irrigated radiofrequency ablation in adult patients.
Ann. Thorac. Surg.. 2006;82:1327-1331,
Abstract | **Full Text** | **PDF**

Efficacy and safety of right and left atrial ablations on the beating heart with irrigated bipolar radiofrequency energy: A long-term animal study
J. Thorac. Cardiovasc. Surg.. 2006;132:853-860,
Abstract | **Full Text** | **PDF**

Cavotricuspid isthmus angiography predicts atrial flutter ablation efficacy in 281 patients randomized between 8 mm- and externally irrigated-tip catheter
Eur Heart J. 2006;27:1833-1840,
Abstract | **Full Text** | **PDF**

Comparison of Electrode Cooling Between Internal and Open Irrigation in Radiofrequency Ablation Lesion Depth and Incidence of Thrombus and Steam Pop
Circulation. 2006;113:11-19,
Abstract | **Full Text** | **PDF**

Discrepancies Between Catheter Tip and Tissue Temperature in Cooled-Tip Ablation: Relevance to Guiding Left Atrial Ablation
Circulation. 2005;112:954-960,
Abstract | **Full Text** | **PDF**

Where to draw the mitral isthmus line in catheter ablation of atrial fibrillation: histological analysis
Eur Heart J. 2005;26:689-695,
Abstract | **Full Text** | **PDF**

Atrial Flutter After Surgical Radiofrequency Ablation of the Left Atrium for Atrial Fibrillation
Ann. Thorac. Surg.. 2005;79:108-112,
Abstract | **Full Text** | **PDF**

Indication of the radiofrequency induced lesion size by pre-ablation measurements
Europace. 2005;7:525-534,
Abstract | **Full Text** | **PDF**

Analysis of Catheter-Tip (8-mm) and Actual Tissue Temperatures Achieved During Radiofrequency Ablation at the Orifice of the Pulmonary Vein
Circulation. 2004;110:2988-2995,
Abstract | **Full Text** | **PDF**

A possible surgical technique to avoid esophageal and circumflex artery injuries using radiofrequency ablation to treat atrial fibrillation
ICVTS. 2004;3:352-355,
Abstract | **Full Text** | **PDF**

A possible surgical technique to avoid esophageal and circumflex artery injuries using radiofrequency ablation to treat atrial fibrillation
Interact CardioVasc Thorac Surg. 2004;3:352-355,
Abstract | **Full Text** | **PDF**

Prospective randomised comparison of irrigated-tip and large-tip catheter ablation of cavotricuspid isthmus-dependent atrial flutter
Eur Heart J. 2004;25:963-969,
Abstract | **Full Text** | **PDF**

Catheter Ablation of Ventricular Epicardial Tissue: A Comparison of Standard and Cooled-Tip Radiofrequency Energy
Circulation. 2004;109:2363-2369,
Abstract | **Full Text** | **PDF**

Typical atrial flutter ablation outcome: correlation with isthmus anatomy using intracardiac echo 3D reconstruction
Europace. 2004;6:407-417,
Abstract | **Full Text** | **PDF**

A comparison of open irrigated and non-irrigated tip catheter ablation for pulmonary vein isolation
Europace. 2004;6:330-335,
Abstract | **Full Text** | **PDF**

A new device for beating heart bipolar radiofrequency atrial ablation
J. Thorac. Cardiovasc. Surg.. 2003;126:1859-1866,
Abstract | **Full Text** | **PDF**

An Underrecognized Subepicardial Reentrant Ventricular Tachycardia Attributable to Left Ventricular Aneurysm in Patients With Normal Coronary Arteriograms
Circulation. 2003;107:2702-2709,
Abstract | **Full Text** | **PDF**

Comparison of epicardial and endocardial linear ablation using handheld probes
Ann. Thorac. Surg.. 2003;75:543-548,
Abstract | **Full Text** | **PDF**

Treatment of long-duration atrial fibrillation by modified maze procedure
JRSM. 2002;95:552-553,
Full Text | **PDF**

Catheter ablation using very high frequency current: effects on the atrioventricular junction and ventricular myocardium in sheep
Europace. 2002;4:69-75,
Full Text | **PDF**

Primary closed cooled tip ablation of typical atrial flutter in comparison to conventional radiofrequency ablation
Europace. 2002;4:265-271,
Abstract | **PDF**

Saline-irrigated, cooled-tip radiofrequency ablation is an effective technique to perform the Maze procedure
Ann. Thorac. Surg.. 2001;72:S1090-1095,
Abstract | **Full Text** | **PDF**

Saline-Cooled Versus Standard Radiofrequency Catheter Ablation for Infarct-Related Ventricular Tachycardias
Circulation. 2001;103:1858-1862,
Abstract | **Full Text** | **PDF**

Electrochemical potentials during radiofrequency energy delivery: a new method to control catheter ablation of arrhythmias
Europace. 2001;3:201-207,
Abstract | **PDF**

Efficacy and Safety of an Irrigated-Tip Catheter for the Ablation of Accessory Pathways Resistant to Conventional Radiofrequency Ablation
Circulation. 2000;102:2565-2568,
Abstract | **Full Text** | **PDF**

Electromagnetic Versus Fluoroscopic Mapping of the Inferior Isthmus for Ablation of Typical Atrial Flutter : A Prospective Randomized Study
Circulation. 2000;102:2082-2086,
Abstract | **Full Text** | **PDF**

Radiofrequency Energy-Induced Heating of Bovine Articular Cartilage Using a Bipolar Radiofrequency Electrode
Am J Sports Med. 2000;28:720-724,
Abstract | **Full Text** | **PDF**

Catheter ablation of ventricular tachycardia in patients with structural heart disease using cooled radiofrequency energy: Results of a prospective multicenter study
J Am Coll Cardiol. 2000;35:1905-1914,
Abstract | **Full Text** | **PDF**

Prospective Randomized Comparison of Irrigated-Tip Versus Conventional-Tip Catheters for Ablation of Common Flutter
Circulation. 2000;101:772-776,
Abstract | **Full Text** | **PDF**

Radiofrequency catheter ablation of inappropriate sinus tachycardia guided by activation mapping
J Am Coll Cardiol. 2000;35:451-457,
Abstract | **Full Text** | **PDF**

Lesion Dimensions During Temperature-Controlled Radiofrequency Catheter Ablation of Left Ventricular Porcine Myocardium : Impact of Ablation Site, Electrode Size, and Convective Cooling
Circulation. 1999;99:319-325,
Abstract | **Full Text** | **PDF**

The Thermal Effect of Monopolar Radiofrequency Energy on the Properties of Joint Capsule: An In Vivo Histologic Study Using a Sheep Model
Am J Sports Med. 1998;26:808-814,
Abstract | **Full Text** | **PDF**

Successful Irrigated-Tip Catheter Ablation of Atrial Flutter Resistant to Conventional Radiofrequency Ablation
Circulation. 1998;98:835-838,
Abstract | **Full Text** | **PDF**

Inverse Relationship Between Electrode Size and Lesion Size During Radiofrequency Ablation With Active Electrode Cooling
Circulation. 1998;98:458-465,
Abstract | **Full Text** | **PDF**

Subendocardial and Intramural Temperature Response During Radiofrequency Catheter Ablation in Chronic Myocardial Infarction and Normal Myocardium
Circulation. 1997;95:2155-2161,
Abstract | **Full Text**

Low-Temperature Mapping Predicts Site of Successful Ablation While Minimizing Myocardial Damage
Circulation. 1996;94:253-257,
Abstract | **Full Text**

Thermal Latency in Radiofrequency Ablation
Circulation. 1996;93:1083-1086,
Abstract | **Full Text**

Electrophysiological Effects of Catheter Ablation of Inferior Vena Cava Tricuspid Annulus Isthmus in Common Atrial Flutter
Circulation. 1996;93:284-294,
Abstract | **Full Text**

Characterization of Reentrant Circuits in Left Atrial Macroreentrant Tachycardia: Critical Isthmus Block Can Prevent Atrial Tachycardia Recurrence
Circulation. 2002;105:1934-1942,
Abstract | **Full Text** | **PDF**